NATIONAL ADVISORY COMMITTEE FOR AERONAUTICS

TECHNICAL MEMORANDUM

No. 1108

FORCE AND PRESSURE-DISTRIBUTION MEASUREMENTS

ON A RECTANGULAR WING WITH A SLOTTED DROOP NOSE

AND WITH EITHER PLAIN AND SPLIT FLAPS IN

COMBINATION OR A SLOTTED FLAP

By H. G. Lemme

Translation

Kraftmessungen und Druckverteilungsmessungen an
einem Rechteckflugel mit Spaltknicknase,
Wolbungs – und Spreizklappe oder Rollklappe

Forschungsbericht Nr. 1676/2

Washington

March 1947

NATIONAL ADVISORY COMMITTEE FOR AERONAUTICS

TECHNICAL MEMORANDUM NO. 1108

FORCE AND PRESSURE-DISTRIBUTION MEASUREMENTS

ON A RECTANGULAR WING WITH A SLOTTED DROOP NOSE

AND WITH EITHER PLAIN AND SPLIT FLAPS IN

COMBINATION OR A SLOTTED FLAP*

By H. G. Lemme

SUMMARY

Part II

In continuation of the investigation presented in
(1), force measurements, and pressure distribution measure-
ments on the midsection, were made on a rectangular wing
with slotted droop nose and end plates, on which could
be placed a choice of either a plain flap-split flap com-
bination or a slotted flap.

The maximum lift increase, due to droop nose
deflection alone, amounted to $\Delta c_{a_{max}} = 0.32$. It is
smaller than the value ($\Delta c_{a_{max}} = 0.55$) obtained for a wing
with simple droop nose. The maximum lift increases
obtained by deflection of the slotted droop nose and
simultaneous flap deflections are smaller than those that
occurred with the corresponding model configurations with
a simple droop nose. This is attributable to the fact
that the absolute value of the low pressure points at the
droop is greater for deflection of the slotted droop nose
than for deflection of the simple droop nose. The
separation of flow is favored. The slotted droop nose
has no particular advantage over the simple droop nose.

I. INTRODUCTION

The measurements on a rectangular wing with simple droop nose, slat, trailing-edge flap and split flap (1) yielded, through a droop-nose installation, a maximum lift increase of $\Delta c_{a_{max}} = 0.55$ nearly equal in significance to the one that occurs with an extended slat. However, with it there occurred at the droop-nose hinge a noticeable low-pressure point, that favored the separation of flow on the surface of the airfoil.

In connection with these measurements investigations should be made to determine whether or not a droop nose, that produces a slot between the droop nose and the airfoil in the deflected position, to be designated briefly as "slot-droop nose" in the following discussion, diminishes the absolute value of the low-pressure point, and thereby makes possible an increase in maximum lift[1].

In this connection, force measurements without boundary layer interference were made on a rectangular wing on which either a trailing-edge flap and a split flap or a slotted flap could be installed. The pressure distribution on a representative cross section of the wing was also determined for various model configurations.

II. MODEL DESCRIPTION

In order to obtain a good comparison with the measurements given in (I) a rectangular wing was also employed in the present case, equipped with end plates, profile NACA 0009-E 4 with chord $l = 0.5m$ and span $b = 1.2$. (See illustration 1.) In consideration of the end plates (H = 0.740m), the effective aspect ratio was $\Lambda = 5$.

The droop nose extending over the entire span of the wing could be deflected in the range from $0°$ to $45°$. Thereby a slot was opened, between wing and droop nose, that enlarged with increasing droop-nose deflection.

[1]The experiments were undertaken, at the suggestion of Mr. Voigt, Department Head of the Messerschmitt Firm that hold the patent on the various forms of the droop nose. (Patent No. 725 768.)

The wing was equipped with the usual trailing-edge flap and split flap from (1), that stretched over the entire span.

Upon deflection η_W of the trailing-edge flap, the rotation point of the split flap moved in a circular arc around the rotation point of the trailing-edge flap. On that account the split flap angle η_S was measured relative to the chord of the trailing-edge flap. In place of the trailing-edge flap and split flap, a slotted flap could be used whose position and deflection angle were selected according to the values previously mentioned in (2).

At the average cross section of the wing, pressure measurements were found whose location and corresponding $\frac{x}{l}$ values are evident in illustration 1.

III. THE MEASUREMENTS AND THEIR EVALUATION

The research was conducted in wind tunnel I of the AVA, which has a stream diameter of 2.25m.

The definitions and symbols agree with the DIN-Standard (DIN L 100, second release 1939). Other definitions that were needed are presented in illustration I.

The (relative) length is $l = 0.5m$

The (relative) area $\quad F = 0.6m^2$

The reference axis for the pitching moment lies at the one-quarter-chord point.

(1) Force measurements for $R_{eff} = 1.2 \times 10^6$ ($v \approx 31$ m/s)

The influence of the droop-nose deflections, without flap deflections, on lift, drag and pitching moment was measured next. Then three-component measurements were made with various deflections of trailing-edge flap and split flap for the droop-nose angle deflection most favorable to the maximum lift. The same measurements were also made with a slotted flap in extended and retracted positions.

(2) Pressure-distribution measurements.- The pressure-distribution measurements were made in the "gesunden Strömmung" region. The deflections of the droop nose, as well as those of the trailing-edge flap, were varied. In addition, measurements were made for various droop-nose deflections with slotted flap in both extended and retracted positions.

For illustration purposes the pressure-distribution measurements at several angles of the attack are reproduced in illustrations 4 to 8.

The local pressures p corresponding to the dynamic pressure q were plotted as directly projected on to the wing chord line. The pressures on the plain and split flaps were projected from their true deflections, while the pressures for the droop nose and slotted flap were plotted as if they were always at zero deflection but were shifted slightly upstream or downstream.

To determine the tangential force of the droop nose, the local pressure p corresponding to the dynamic pressure q was projected on a perpendicular to the chord line of the droop nose. These graphs are not presented in this publication.

In one part of the experiment the pressure measuring points, in the slot of the droop nose, leaked. Since the graphs of the curves $\frac{p}{q} = f\left(\frac{x}{l}\right)$ at these points are almost independent of flap deflection for like droop-nose deflections and like angles of attack, - in order to avoid repetition of the measurements - they were drawn in the same manner as the curves for like droop-nose deflections and like angles of attack with similar flap deflections. For deflected plain and split flaps in combination, as in (1), graph of the curves, $\frac{p}{q} = f\left(\frac{x}{l}\right)$ for the inboard portion of the flap was marked to correspond to the measurements indicated in (3). The curves so obtained were used as the basis of the following integrations:

It is

p_u static pressure on the under side of the wing

p_o static pressure on the upper side of the wing

$$\Delta p = p_u - p_o$$

b span

l_{Kn} relative length of the droop nose

$F_{Kn} = b \times l_{Kn}$ relative area of the droop nose

It means: index D determined from pressure measurements

$c_{n_{Kn}}$ normal-force coefficient of the droop nose perpendicular to the chord line of the droop nose based on the droop-nose area

$c_{t_{Kn}}$ tangential-force coefficient of the droop nose parallel to the chord line of the droop nose based on the droop-nose area

c_{Kn_1} the moment coefficient of the droop nose, resulting from the normal force, around its axes of reference based on droop-nose area and droop-nose length

c_{Kn_2} the moment coefficient of the droop nose resulting from the tangential force around its axis of reference based on droop-nose area and droop-nose length.

c_{Kn} the total moment coefficient of the droop nose around its axes of reference based on droop-nose area and droop-nose length
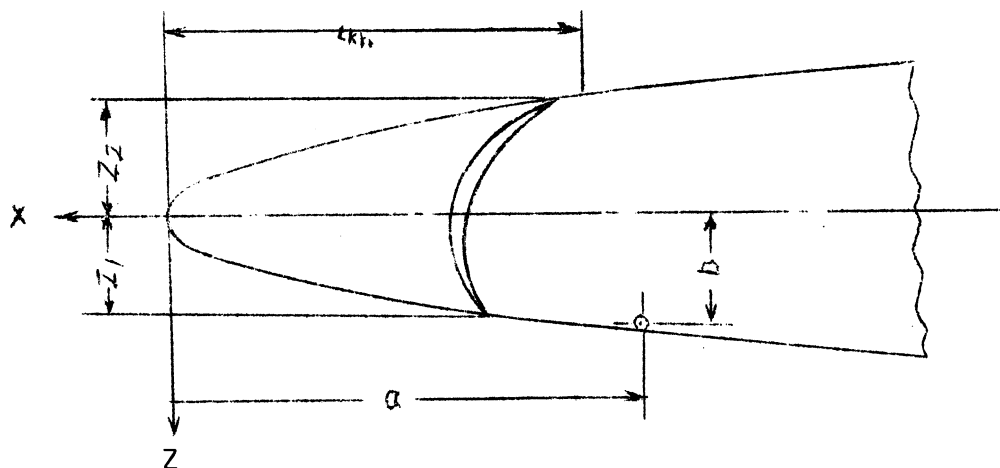
$$c_{n_{Kn_D}} = \frac{1}{l_{Kn}} \int_{l_{Kn}}^{0} \frac{\Delta p}{q} \, dx$$

$$c_{t_{Kn_D}} = \frac{1}{l_{Kn}} \int_{z_2}^{z_1} \frac{\Delta p}{q} \, dx$$

$$c_{Kn_{1_D}} = \frac{1}{l_{Kn}^2} \int_{l_{Kn}}^{0} \frac{\Delta p}{q} \, x \, dx + \frac{a}{l_{Kn}^2} \int_{l_{Kn}}^{0} \frac{\Delta p}{q} \, dx$$

$$c_{Kn_{2_D}} = \frac{1}{l_{Kn}^2} \int_{z_2}^{z_1} \frac{\Delta p}{q} \, z \, dz + \frac{b}{l_{Kn}^2} \int_{z_2}^{z_1} \frac{\Delta p}{q} \, dz$$

$$c_{Kn_D} = c_{Kn_{1_D}} + c_{Kn_{2_D}}$$

IV. EXPERIMENTAL RESULTS

1. Force Measurements

A maximum lift increase of $\Delta c_{a_{max}} = 1.07$ was obtained by extension of the slotted flap without droop-nose deflection. (Illustration 3.) For the same extensions a maximum lift increase of $\Delta c_{a_{max}} = 1.27$ may be found in (2) for a wing of profile NACA 23012 with $R_{eff} = 8.0 \times 10^6$. The difference is atributable to the larger Reynolds number as well as to the profile.

Without plain and split-flap deflections, the largest maximum lift increase $\Delta c_{a_{max}} = 0.32$, occurred with a droop-nose angle $\delta = 25^\circ$ (illustration 2), while without slotted-flap deflection a $\Delta c_{a_{max}}$ value of 0.34 was obtained for a droop-nose angle of 30°. The differences in the maximum lift increase and in the droop-nose angle is attributed to the various effects of flap slots.

A droop-nose angle amounting to $\delta = 35^\circ$ with simultaneous flap deflections, yielded the greatest maximum lift increase. This value of δ is greater than the value ($\delta = 30^\circ$) for the simple droop nose. It is independent of the various flap deflections.

The influence of droop-nose deflection on drag and pitching moment were discussed in detail in (1). This influence is nearly the same for deflection of the slotted droop nose.

The resulting maximum lifts are found in table I. For similar model configurations the increments are smaller for the slotted droop nose than for the simple droop nose. The explanation for this can be found in the discussion of the pressure-distribution measurements. The angles of attack corresponding to the maximum lift values are 2° smaller for the slotted droop nose without deflection and 5° smaller with flap deflection than for the simple droop nose.

The largest maximum lift increase $\Delta c_{a_{max}} = 1.508$ was obtained with extended slotted flap and a deflection angle ($\delta = 35^\circ$) of the slotted droop nose. This maximum lift increase is attributable largely to the deflection of the slotted flap.

In contrast to the simple wing, the maximum lift increase, resulting from deflection of the slotted droop nose with simultaneous flap deflections, $\eta_w = 20^\circ$ and $\eta_s = 40^\circ$ is larger than it is without flap deflections.

2. Pressure Measurements

Since the various pressure measuring points must have a finite distance from one another it is not safe to proceed without also measuring the actually existing low-pressure points.

A comparison of pressure measurements for the simple droop nose (1) and for the slotted droop nose (illustrations 4 to 8) with the same model configurations and with approximately the same angle of attack demonstrated that the flow on the surface of the slotted droop nose begins to separate for small droop-nose angles, as it did on the surface of the simple droop nose. Furthermore, the absolute values of the low-pressure points at the droop of the slotted droop nose are noticeably larger than at the droop of the simple droop nose. It follows that the separation of flow on the surface of the airfoil was favored. Consequently the maximum lift for the deflected slotted droop nose is smaller than for the deflection of the simple droop nose.

The normal-force, tangential-force, and moment coefficients $\left(c_{n_{Kn_D}}, c_{t_{Kn_D}}, c_{Kn_D} \right)$ that were obtained through integration from the pressure-distribution measurements, were recorded for the various model configurations and angles of attack, independently of the droop-nose angle δ. (Illustrations 9 to 23.) The shape of the curves, which resembled those for the simple droop nose, is discussed in (1). For the same model configurations the normal force is smaller, the absolute value of the tangential force and the moment are larger for the slotted droop nose than for the simple droop nose. However, the differences are not very great.

3. Conclusions

For large droop-nose deflections and angles of attack, the air flow resulting from the slot between droop nose and wing, should retard friction layers on the surface of the airfoil.

The low-pressure points at the droop of the droop nose should also be reduced by the slotted droop nose.

The wind-tunnel measurements did not verify these decreases. A slot effect is not recognizable. In contrast to the simple droop nose, the droop-nose angle most favorable to maximum lift is no longer the same with and without flap deflection. The low-pressure points at the droop of the droop nose were greater for deflection of the slotted droop nose than for deflection of the simple droop nose and favored rather than delayedd the separation of flow on the surface of the airfoil. For like model configurations, the maximum lift obtained for a wing with slotted droop nose is smaller than the one obtained for a wing with simple droop nose. The slotted droop nose has no advantage over the simple droop nose.

Translated by Douglas Aircraft Company, Inc.

REFERENCES

1. Lemme, H. G.:   Force Measurements and Pressure
        Distribution Measurements on a Wing with Droop
        Nose, Slot, Trailing Edge Flap and Split Flap.
        FB 1676.

2. Wenzinger, C. J. and Harris, T. A.:   Wind-Tunnel
        Investigation of an NACA 23012 Airfoil with
        Various Arrangements of Slotted Flaps.
        NACA Rep. 664 (1939).

3. Schrenk, O.:   Pressure and Speed Distribution Along
        the Wing Chord for Various States of Flight,
        Ringbuch der Luftfahrttechnik Bd I, A 11.
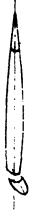
Section	Droop nose angle δ	Angle of the			Angle of attack $\alpha_{ca\,max}$	Maximum lift $c_{a\,max\,ges}$	Total increase of the maximum lift $\Delta c_{a\,max\,ges}$	Increase of the maximum lift by flap deflection $\Delta c_{a\,max\,Kl}$	Increase of the maximum lift by droop nose deflection $\Delta c_{a\,max\,Kn}$
		Trailing edge flap η_W	Split flap η_S	Roll flap η_R					
	0	—	—	Basic profile	12,2	0,720	—	—	—
	0	0	—	50	7,5	1,789	1,069	1,069	—
	25	—	0	—	19,4	1,049	0,320	—	0,320
	30	0	60	0	18,8	1,061	0,344	—	0,344
	35	20	40	—	19,6	1,832	1,112	0,756	0,356
	35	10	50	—	16,6	1,785	1,065	0,831	0,234
	35	—	—	—	17,9	1,901	1,481	0,820	0,361
	35	—	—	50	16,6	2,228	1,508	1,069	0,439

Table 1. Compilation of the maximum lifts.

Fig. 1   NACA TM No. 1108

Labels on the figure:

- $\eta_W = 10$
- $\eta_S = 50°$
- $\eta_R = 50°$
- $0.2\,l$
- $0.25\,l$
- $0.07\,l$
- $l = 500$
- N.A.C.A. 0009 – E4
- 14.7
- $y_{Kn} = 0.054$
- $\frac{x}{l}$
- $0.125\,l$
- $\delta = 35°$
- $+C_{Kn}$
- $+C_M$
- Axis of reference for the longitudinal moment
- Line of reference for the angle of attack
- Axis of reference for the moment of the droop nose
- O = Points of pressure measurement

	21	22	23	24	25	26	27	28	29	30	31	32	33	34	35	36	37	38	39	40	41	42	43
Points of measurement, upper surface / lower	1	2	3	4	5						6	7			8	9	10	11	12	13	14	15	16
	44	67	45	46	47	48	49	50	51	52	53	54	65	66	68	69	70	71	72	73	64		
Points of measurement, upper / lower	17	18	19	20	47	48	55	51	52	53	54	58	57	58	60	61	68	69	70	71	72	73	64
												56	59	59									
$\frac{x}{l}$	-0,012	-0,029	-0,05	-0,075	-0,093	-0,094	-0,082	-0,073	-0,075	-0,078	-0,083	-0,088	-0,094	-0,11	-0,125	-0,15	-0,2	-0,25	-0,3	-0,4	-0,5	-0,6	-0,7
$\frac{x}{l}$	-0,744	-0,8	-0,081	-0,9	-0,95	-0,749	-0,749	-0,752	-0,77	-0,785	-0,78	-0,76	-0,75	-0,775	-0,79	-0,0825	-0,83	-0,85	-0,0875	-0,9	-0,93	-0,095	-0,0995

Figure 1.

Figure 2. Lift as a function of drag, angle of attack and longitudinal
moment for various model positions.
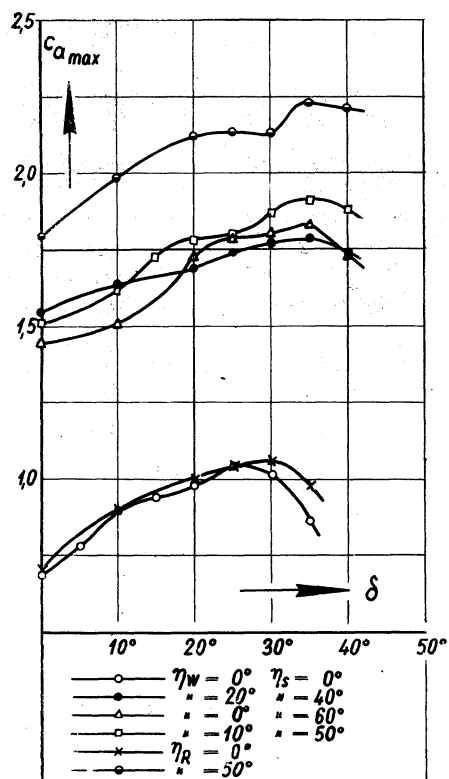
Figure 3. Maximum lift as a function of
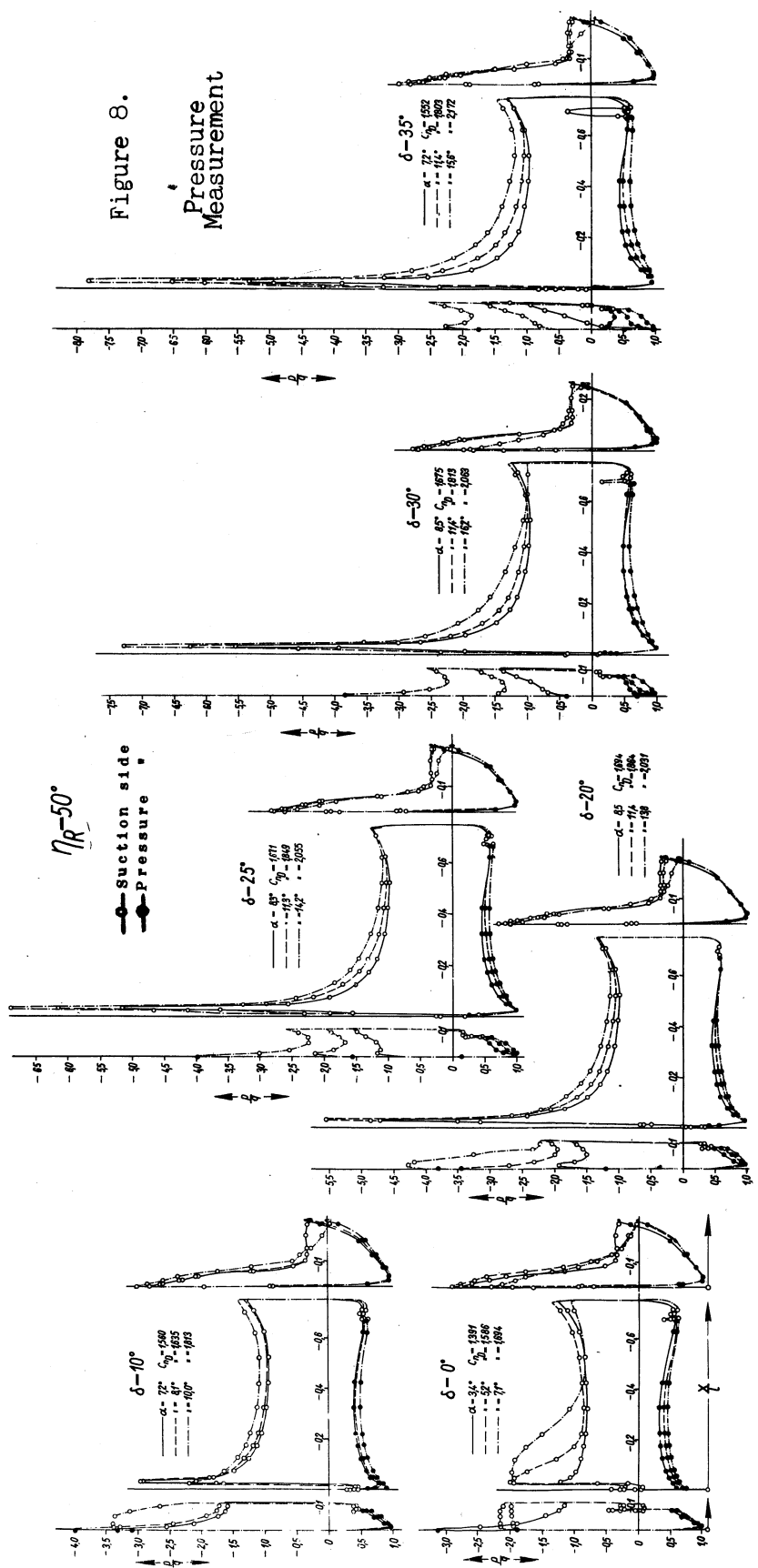the droop nose angle for various flap
positions.

Fig. 4

Figure 4.

Pressure
Measurement

Figure 5.
Pressure Measurement

Fig. 6   NACA TM No. 1108

Figure 6.

Pressure Measurement

$\eta_w = 10°$ $\eta_s = 50°$

Suction side
Pressure "

Figure 7.

Pressure Measurement

Fig. 8   NACA TM No. 1108

Figure 8.

Pressure Measurement
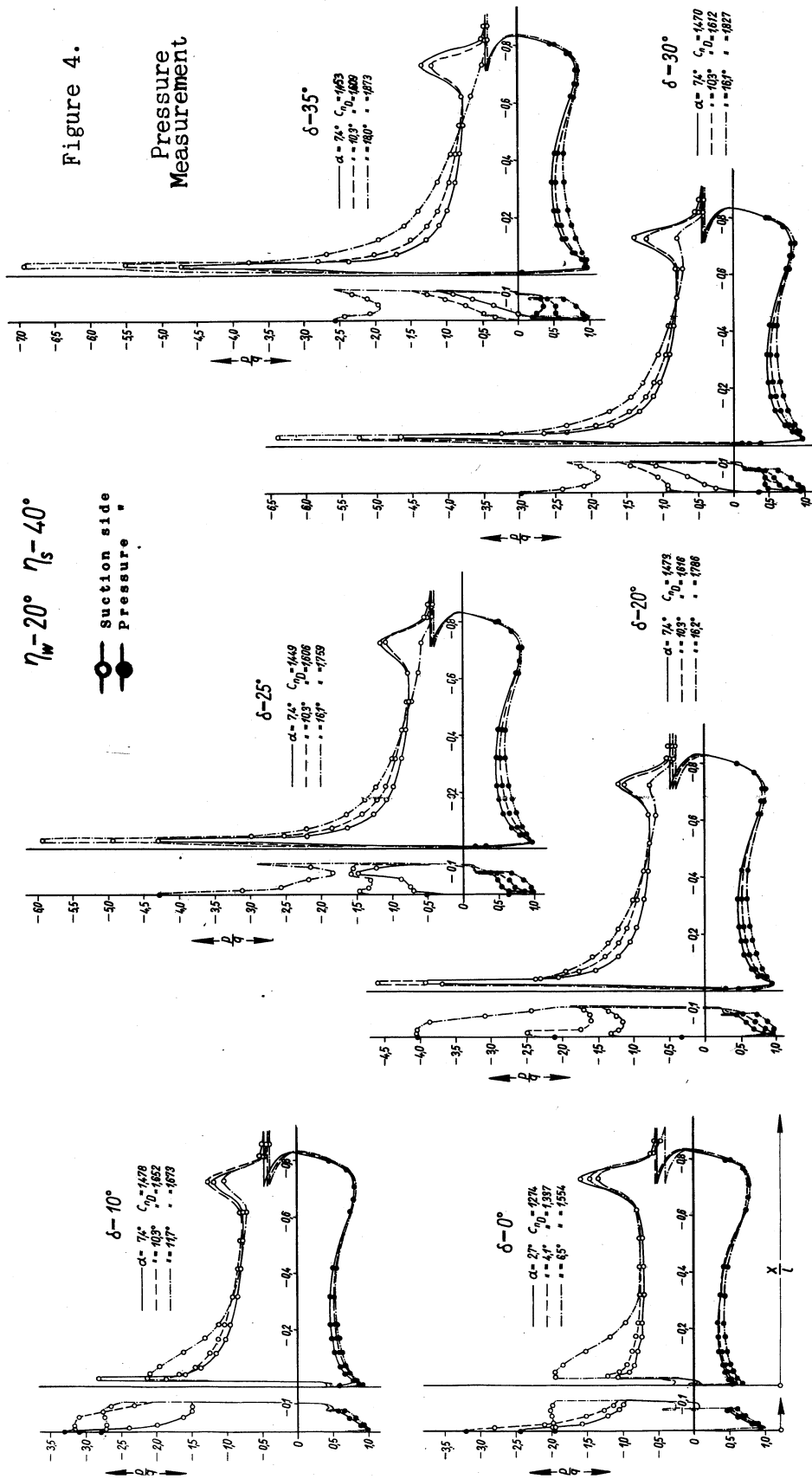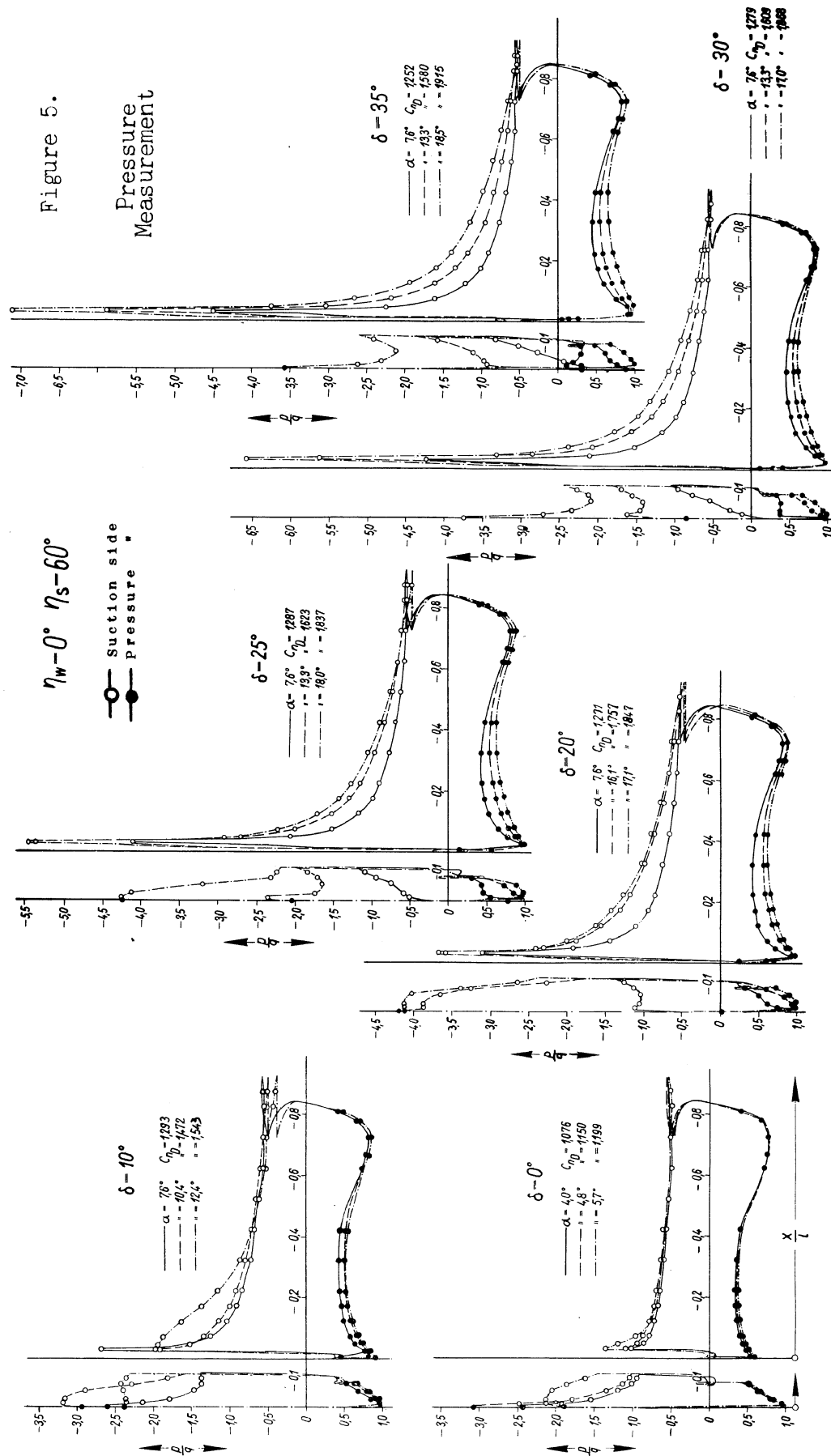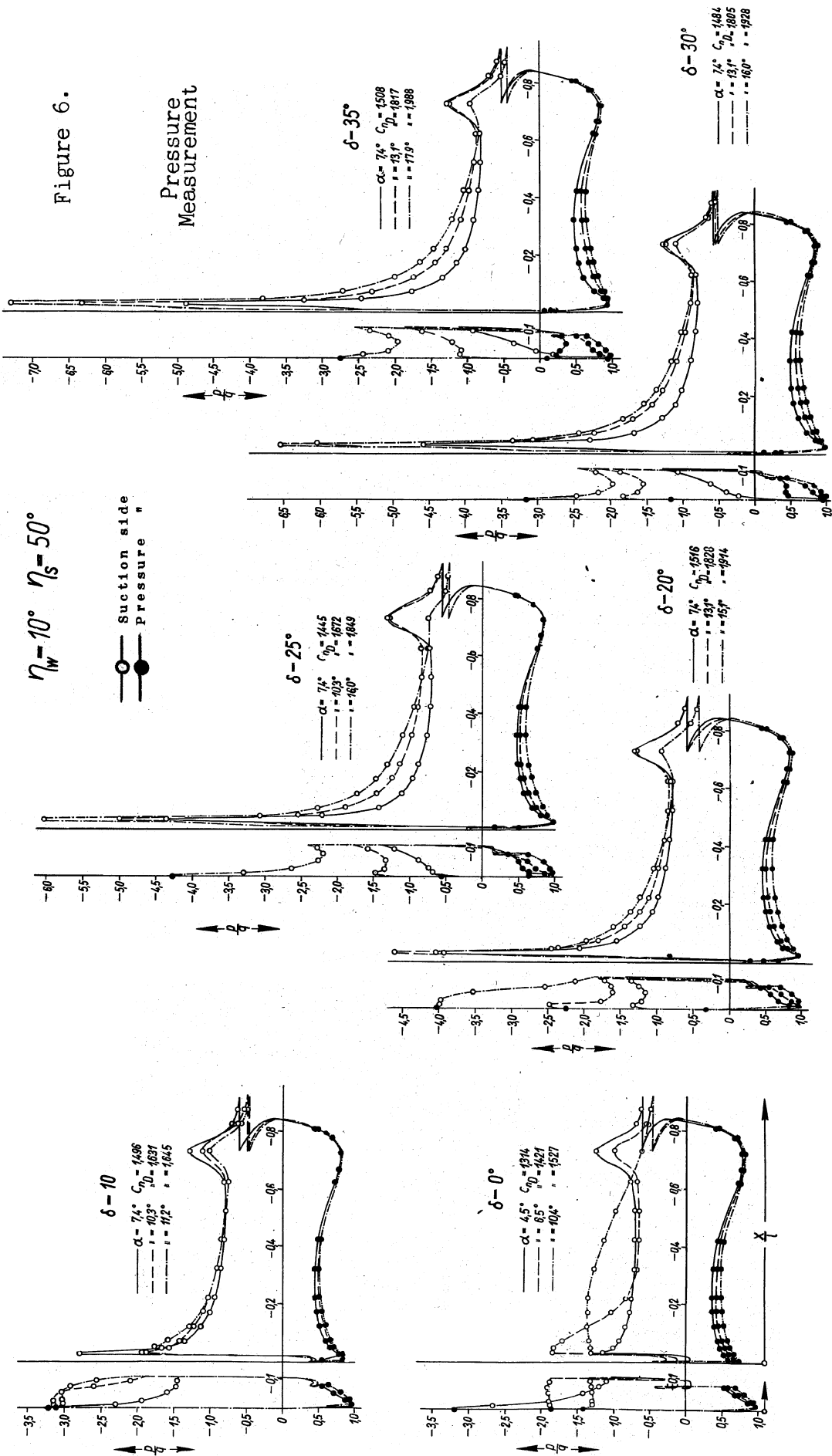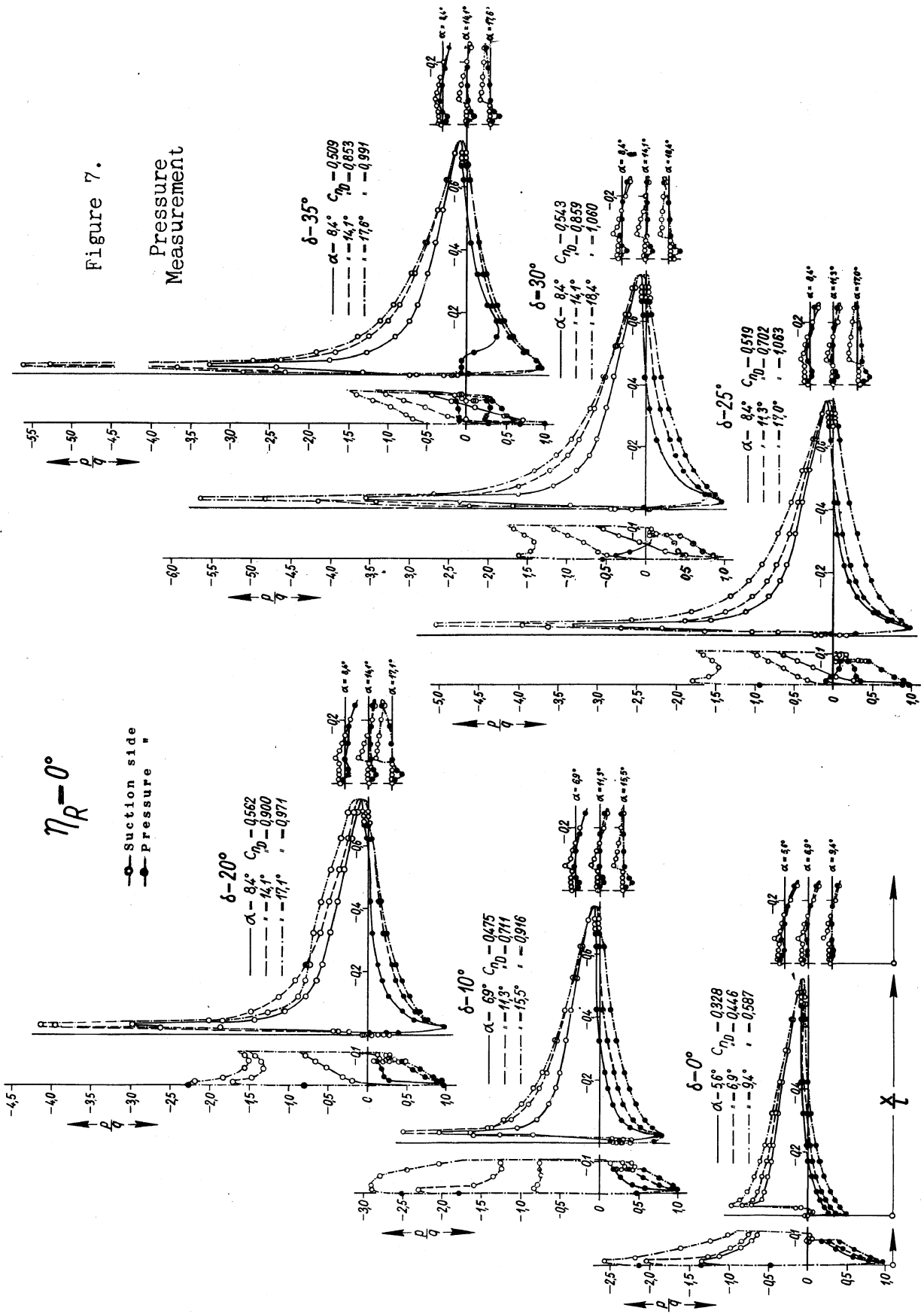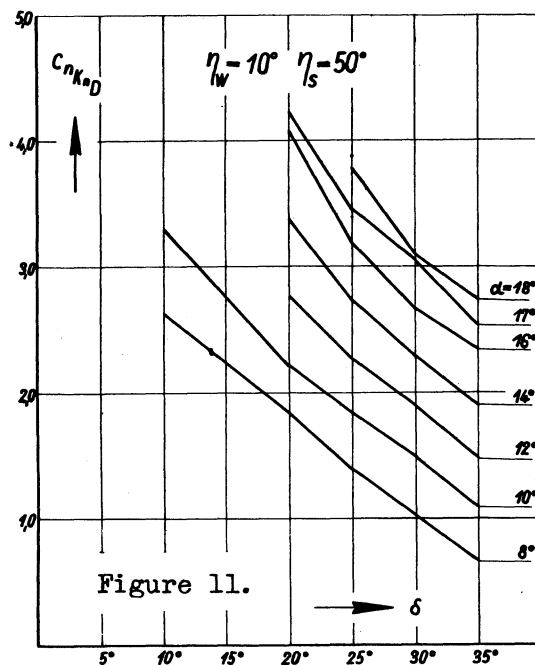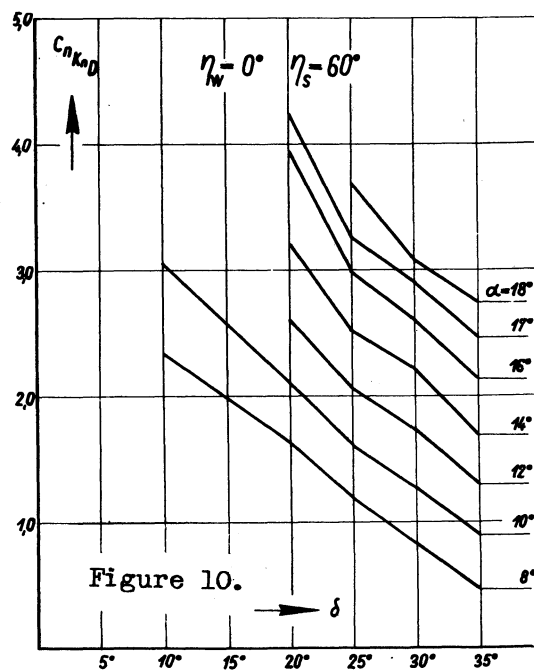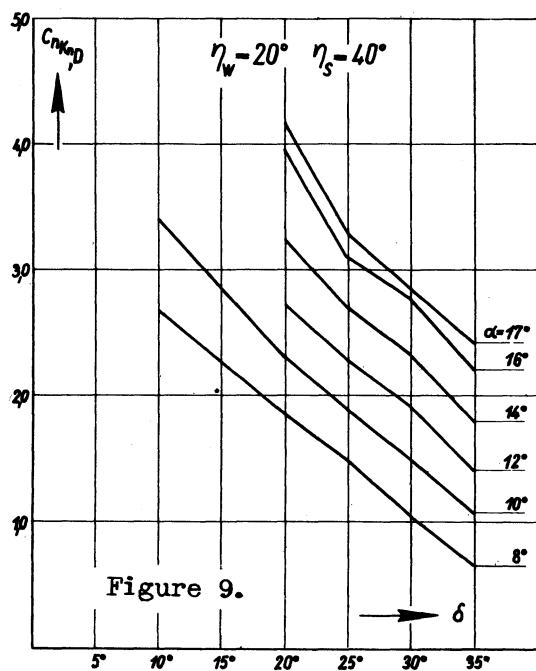
Figures 9 through 11. Normal force coefficient of the droop nose as a function of the droop nose angle at various angles of attack.
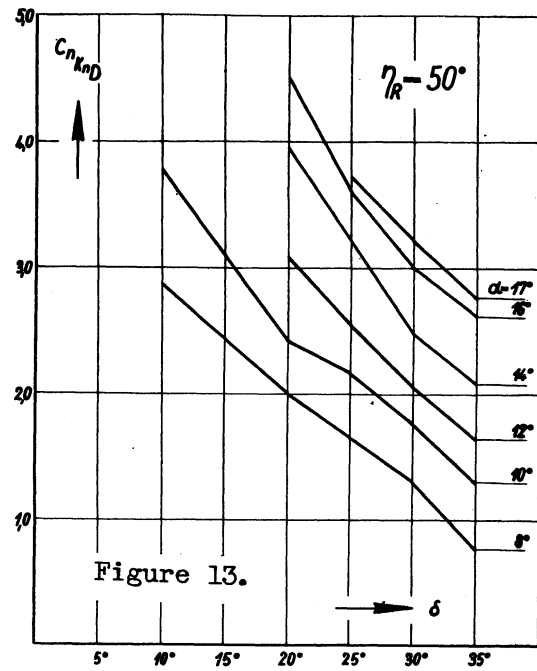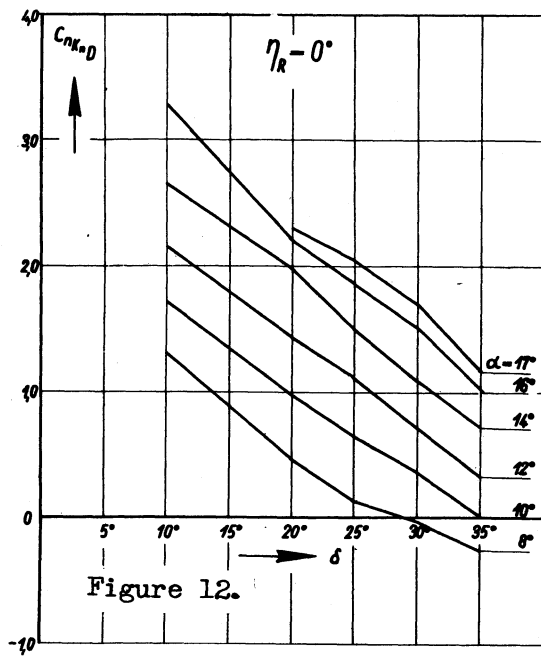
Figures 12 through 13. Normal force coefficient of the droop nose as a function of the droop nose angle at various angles of attack.
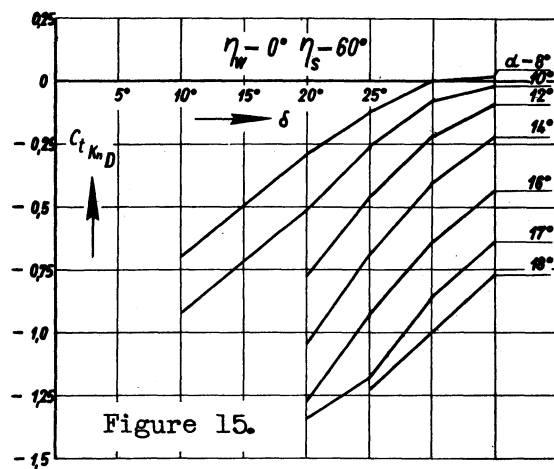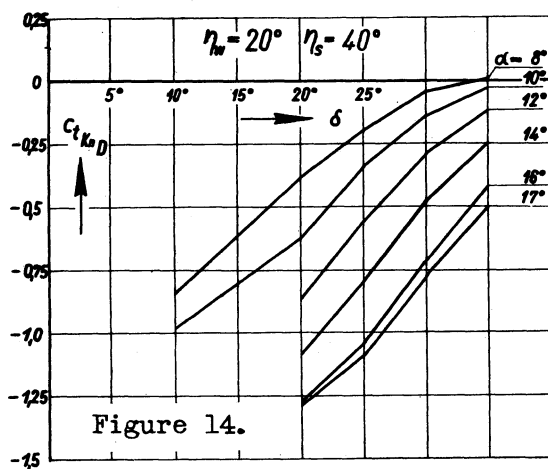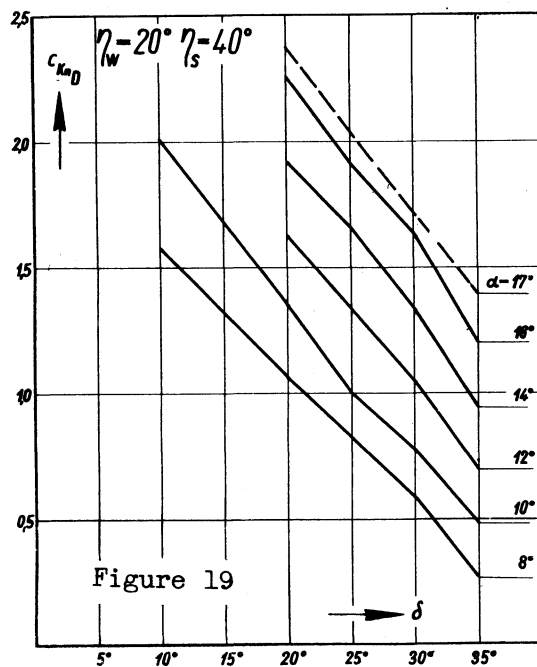

Figure 14 and 15. Tangential force coefficient of the droop nose as a function of the droop nose angle at various angles of attack.
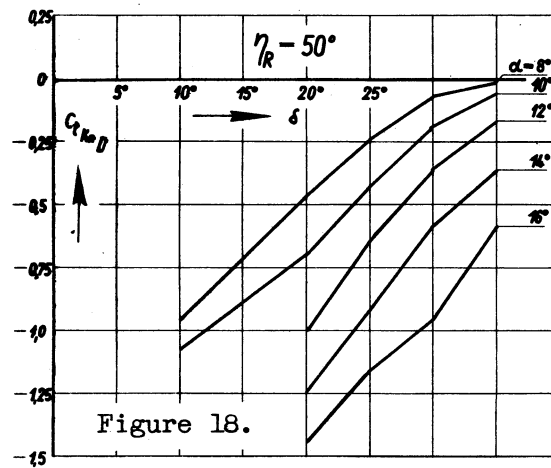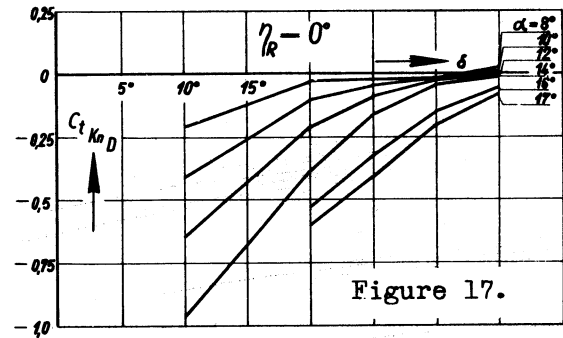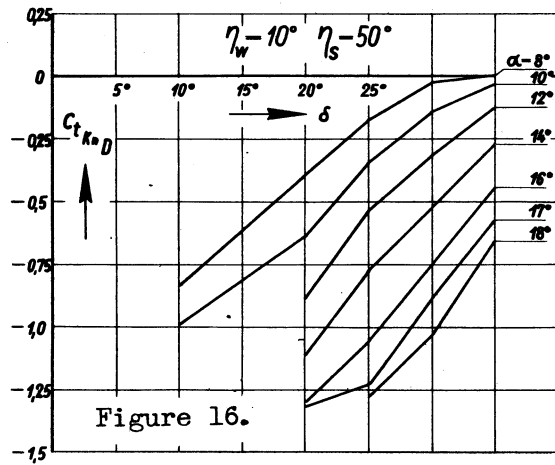
Figures 16 through 18. Tangential force coefficient of the droop nose as a function of the droop nose angle at various angles of attack.
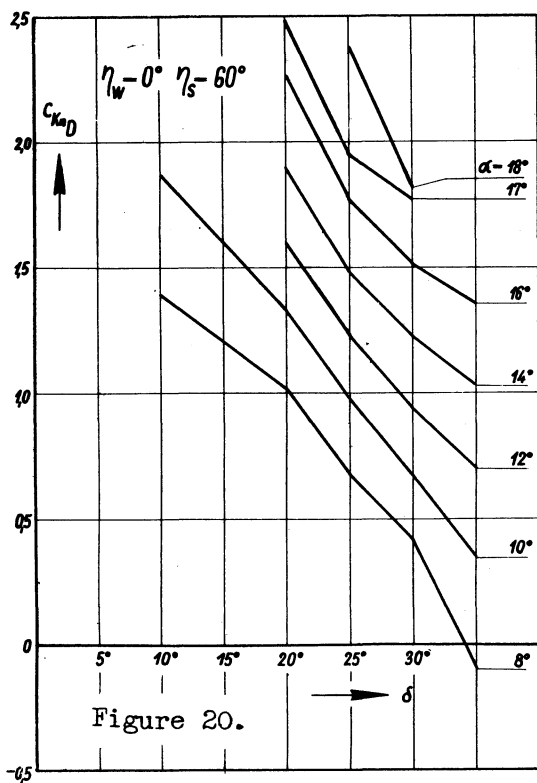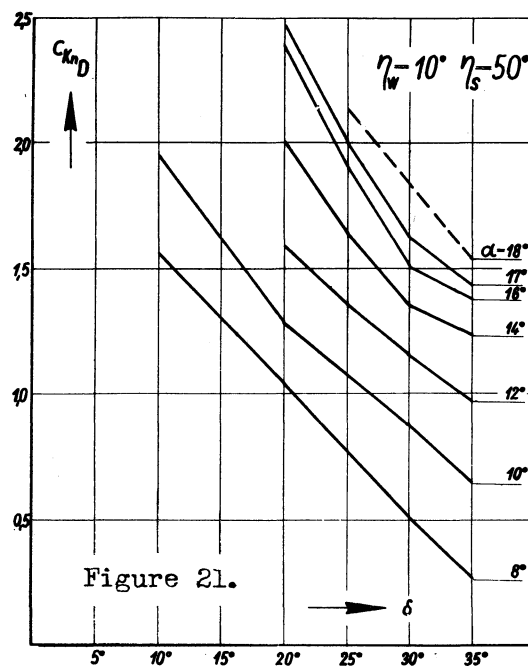
Figure 19

Figure 20.

Figure 21.

Figures 19 through 21. Moment coefficient of the droop nose as a function of the droop nose angle at various angles of attack.
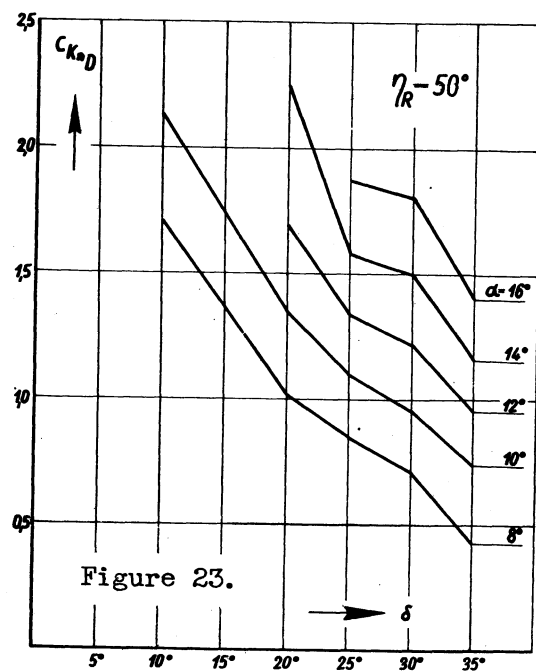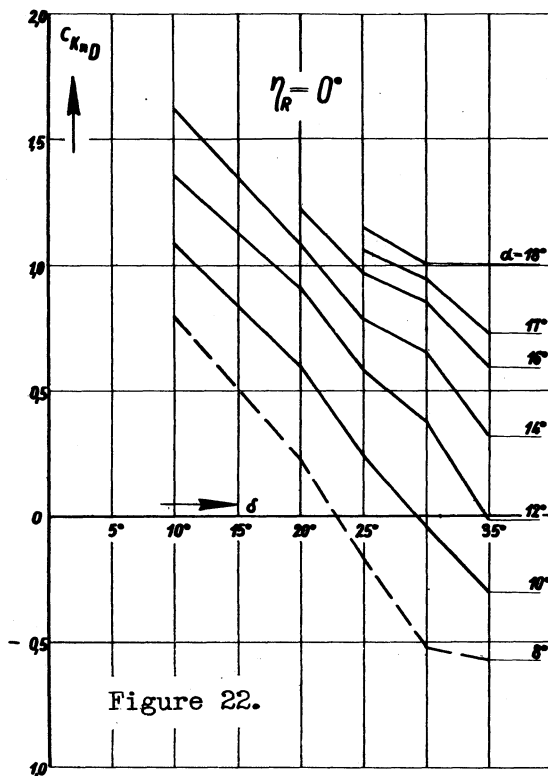
Figure 22 and 23. Moment coefficient of the droop nose as a function of
   the droop nose angle at various angles of attack.